

Soft Matter

Accepted Manuscript



This is an *Accepted Manuscript*, which has been through the Royal Society of Chemistry peer review process and has been accepted for publication.

Accepted Manuscripts are published online shortly after acceptance, before technical editing, formatting and proof reading. Using this free service, authors can make their results available to the community, in citable form, before we publish the edited article. We will replace this *Accepted Manuscript* with the edited and formatted *Advance Article* as soon as it is available.

You can find more information about *Accepted Manuscripts* in the [Information for Authors](#).

Please note that technical editing may introduce minor changes to the text and/or graphics, which may alter content. The journal's standard [Terms & Conditions](#) and the [Ethical guidelines](#) still apply. In no event shall the Royal Society of Chemistry be held responsible for any errors or omissions in this *Accepted Manuscript* or any consequences arising from the use of any information it contains.

ARTICLE

Cite this: DOI: 10.1039/x0xx00000x

Received 00th January 2014,

Accepted 00th January 2014

DOI: 10.1039/x0xx00000x

www.rsc.org/

Swelling Enhancement of Polyelectrolyte Brushes Induced by External Ions

Xiao Chu,^{ab} Jingfa Yang^a Guangming Liu^c and Jiang Zhao^{*a}

It has been observed previously that, when permanently charged polyelectrolyte brushes are exposed to external salt solution, it shrinks when the salt level is high enough. Before the salt concentration gets to that limit, an enhanced swelling process is observed and investigated systematically with a few strong polyelectrolyte brush systems in this study, including sodium polystyrene sulfonate (PSSNa), poly([2-(methacryloyloxy)ethyl] trimethylammonium chloride) (PMETAC) and potassium poly(3-sulfopropyl methacrylate) (PSPMA) with different molecular weight and grafting density, by combination of methods including ellipsometry, quartz crystal microbalance with dissipation (QCM-D) and atomic force microscopy (AFM). The swelling enhancement is expressed by the thickening of the brush layer at moderate salt concentration, accompanied by the decrease of refractive index, the increase of the amount of solvent inside the brushes and the increase of the retardation time. A scenario is proposed that, when the counterions penetrate into the brushes driven by the external salt ions, they disrupt and break up the previously formed multiplets due to the dipole-dipole interaction by the ion-pairs on the polymer chain. The process results in the release of the bound segments and the stretching of the polymer chains.

Introduction

As the important candidates of intelligent materials, polymer gels and brushes have been attracting considerable attention.^{1,2} The former network structure is formed by physical or chemical cross-linking of polymer chains and the latter is formed by end-tethering of polymer chains at surfaces with high enough grafting density. Among these systems, polyelectrolyte gels and brushes have been considered to be very promising for applications in aqueous environment, especially for bio-medical purposes.^{3,4}

Polyelectrolyte brushes are formed by densely grafting polyelectrolyte chains on surfaces.^{2,4} The brushes are swelled to a large extent in aqueous environment and they are subject to change in response to environmental stimuli such as pH value, ionic strength and temperature. Polyelectrolyte brushes are believed to have promising potentials in a number of applications, such as stabilization of colloidal suspensions, fabrication of interfaces with ultra-low friction, etc.^{5,6} They have also been considered as nano-reactors in which different types of external substances (ions and proteins) can be held so that small-scaled reactions can be conducted.⁷

It has been recognized that polyelectrolyte brushes change their swelling extent in response to the change of external salt concentration, for both weak and strong polyelectrolyte brushes. For weak polyelectrolyte brushes (annealed brushes), whose charges rely on the association-dissociation process of the ionizable groups, the maximum swelling at moderate salt concentration has been investigated for a number of systems, such as poly(acrylic acid) (PAA) brushes,⁸⁻¹⁰ poly methacrylic acid (PMAA) brushes¹¹ and poly(2-(diethylamino) ethyl

methacrylate) (PDEA) brushes,¹² by experimental as well as theoretical investigations.¹³ For the permanently charged strong polyelectrolyte brushes (quenched brushes), most studies have mainly focused on the behaviours in high salt concentration regions, where a collapse from “osmotic brushes” to “salted brushes” occurs, and not much attention has been paid to the swelling in relatively low salt concentration regions. Two reports have shown the slight increase of brush’s height at the lower salt concentration before the brush’s collapses at high enough salt level: the cationic poly([2-(methacryloyloxy)ethyl] trimethylammonium chloride) (PMETAC) brushes studied by neutron reflectometry¹⁴ and the other for the cationic poly-4-vinyl (N-methyl-pyridinium) (MePVP) brushes investigated by ellipsometry.¹⁵

In principle, the properties of polyelectrolyte brushes is governed by several factors including the long-range electrostatic interaction, the conformational entropy of the polymer chains, as well as the short-range excluded volume effect.^{5,16} Another important factor is counterions, which has been attracting considerable research efforts in the past decades.^{17,18} One of the widely accepted models is the “confinement of counterions” inside the brushes at high enough grafting density – all of the counterions of the brush are restricted within the brush layer and their osmotic pressure makes the charged chains stretched and, as a consequence, the brushes swelled (the osmotic brushes model). This conclusion was reached based on that the very high surface charge density generates very small value of the Gouy-Chapman length, much shorter than the height of the brushes. However, considering the finite dimension of the brushes, the above argument can be rather simplified. Experimental evidence has been reported on

the segmental density profile along the normal direction of the brush, exposing a non-uniform distribution – a much higher density at the inner part of the brushes than the outer rim and the segment density decays gradually at the top portion of the brushes.^{14,19} Such a non-uniform distribution of chain segments should have a strong impact on the distribution of counterion, and therefore, the distribution of counterions of a real polyelectrolyte brush can be quite different to the theoretical prediction based on the ideal situation. Another important factor affecting the counterion distribution is the presence of external salt (ions) in the solution by which the electrostatic interaction can be affected. According to theory previously developed,^{5,16} the external ions are not considered to be effective to the brushes until its concentration overcomes that of counterions inside the brushes, in which case the osmotic pressure generated by the counterions inside the brush is suppressed by the external ions and the brushes' thickness begins to decrease as a consequence.

Based on the non-uniform distribution of the charged segments of the real polyelectrolyte brushes, the distribution of counterions may also exhibit a different feature under the variation of the external salt level accordingly, compared with the theoretical results.^{5,16} Actually, there has been a recent report showing the brushes' height is affected by the external ions at the salt concentration much lower than that required to suppress the osmotic pressure of the counterions.²⁰ In another investigation studying the in-plane diffusivity of fluorescent counterion probes inside polyelectrolyte brushes, it was discovered that the diffusivity of the counterion probes decreases at very low salt concentration, implying a change of counterion distribution and brushes' structure even under very low external ion levels.²¹

These observations have motivated further careful investigations into the response of the polyelectrolyte brushes to the variation of the external salt level and the possible change of the structure. In the current study, a systematic investigation is carried out into the response of polyelectrolyte brushes to the variation of the salt concentration, using several different brush systems and by a number of methods such as ellipsometry, quartz crystal microbalance with dissipation (QCM-D) and atomic force microscope (AFM). The results expose drastic effects to the brushes by external ions at concentration 1-2 orders of magnitude lower than that for brushes' collapse and the enhancement of swelling of the brushes is observed induced by the addition of external ions.

Experimental section

Materials

Amino-terminated polystyrene (PS-NH₂, $M_n = 120 \times 10^3$ g·mol⁻¹ and 32×10^3 g·mol⁻¹; $M_w/M_n = 1.04$), polystyrene (PS, $M_n = 120 \times 10^3$ g·mol⁻¹ and 33×10^3 g·mol⁻¹; $M_w/M_n = 1.13$ and 1.04) were all purchased from Polymer Source (Québec, Canada). [2-(Methacryloyloxy)ethyl] trimethylammonium chloride (METAC, Sigma Aldrich), 3-sulfopropyl methacrylate, potassium salt (SPMA, Sigma Aldrich), 3-trimethoxysilylpropyl 2-bromo-2-methyl-propionate (TBP,

Gelest), ethyl 2-bromoisobutyrate (2-EBiB, Sigma-Aldrich), 2,2'-bipyridine (bpy, Sigma-Aldrich), 2,2,2-trifluoroethanol (TFE, Sigma-Aldrich) and 5,6-epoxyhexyl triethoxysilane (ETS, Gelest) were used as received. Copper (I) bromide (CuBr) and copper (I) chloride (CuCl) were purchased from Sigma-Aldrich and were purified by successive washing with acetic acid and ethanol. Pure sodium chloride (NaCl) and potassium chloride (KCl) were also purchased from Sigma-Aldrich and used as received without any further purification. Deionized water with the resistance of 18.0 MΩ·cm was provided by a Millipore purification system.

Silicon wafers and silica coated crystal sensors were used as substrates for corresponding characterization. Before preparation, they were carefully cleaned by the following successive steps: UV/ozone treatment, ultrasonication in acetone and deionized water, oxygen plasma treatment. By these treatments, the adsorbed organic substances at the substrates' surface are removed and the surfaces are turned to be rich of hydroxyl groups for further modification.

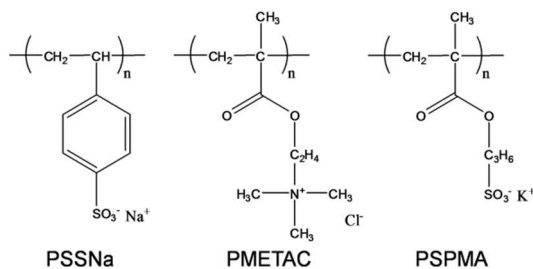
Preparation of sodium polystyrene sulfonate (PSSNa) brushes

The PSSNa brushes were prepared by sulfonation of the PS brushes fabricated by grafting-to method.²² To prepare PS brushes, a self-assembled monolayer of epoxy group terminated silane was firstly prepared on silica substrates and this was done by immersing the substrates in 1wt% cyclohexane solution of 5,6-epoxyhexyl triethoxysilane. Afterwards, a thin film of amino-terminated polystyrene was spin-casted on the pre-coated substrate from its toluene solution with a concentration of 1 wt%. The samples were incubated at 160°C under vacuum for 24 h. Later, the sample was vigorously rinsed with toluene by Soxhlet extraction for 5 h to remove physically adsorbed PS. The grafting density of the PS brushes was adjusted by mixing the reactive PS (amino-terminated PS) with non-reactive PS when the spin-casting was performed. Details of the grafting density adjustment are provided in Supplementary Information.

The PS brushes were sulfonated following a published protocol.²² At first, acetyl sulfate was prepared by adding concentrated sulfuric acid (3.6 mL, 0.064 mol, 95%) to a mixture of acetic anhydride (10.2 mL, 0.108 mol) and 1,2-dichloroethane (49.8 mL) in an ice bath. Then, this mixture was added slowly into a reactor containing PS coated substrates. The reactor was heated to 60°C for 5 h. Afterwards, the reaction was terminated and the sample was rinsed thoroughly with ethanol. By this process, the PS brushes were changed into polystyrene sulfonic acid brushes, which were later neutralized in NaHCO₃ (0.5 M) solution to become polystyrene sulfonate sodium. At the final stage, the PSSNa brushes were rinsed in a Soxhlet extractor in deionized water for 4 h to remove the residual salts and then dried under vacuum for more than 8 h. The degree of sulfonation was estimated to be more than 85% by X-ray photoelectron spectroscopy. The original data of determination of sulfonation is provided in Supplementary Information. The thickness characterization of PSSNa brushes was conducted using an ellipsometer equipped with a liquid sample cell (detailed in later text).

Preparation of other polyelectrolyte brushes

The preparation of other polyelectrolyte brushes, poly([2-(methacryloyloxy)ethyl] trimethylammonium chloride) (PMETAC) and potassium poly(3-sulfopropyl methacrylate) (PSPMA), was carried out by the grafting-from method through the surface-initiated atom transfer radical polymerization (SI-ATRP). Substrates with TBP initiator monolayer were prepared as that with the ETS monolayer. SI-ATRP of PMETAC and PSPMA brushes was conducted following the well-established methods described in literature.^{23,24} To characterize the molecular weight of polyelectrolyte chain, the free initiator (sacrificial initiator) method was employed. The typical polymerization of METAC (or PSPMA) was carried out in TFE/isopropyl alcohol (iPrOH) (20/1, v/v) (or water/dimethylformamide (DMF) (12.5mL/12.5mL)) with a free initiator at 60°C for 48 h (or at 25°C for 19 h) using a reaction system consisting of METAC/bpy/EB/CuBr in the following molar ratios: 1600/8/5/4 (or SPMA/bpy/EB/CuCl/CuCl₂ as 50/5/1/1/1). After the polymerization, the polymer was isolated by extensive dialysis in water and the final solid product was obtained by lyophilization. The silicon wafers were washed with TFE using a Soxhlet apparatus for 12 h to remove the free polymer adsorbed on their surfaces. The samples were dried under vacuum for 24 h. The chemical structures of three types of polyelectrolyte brushes studied in the current study are shown in Scheme 1.



Scheme 1 The chemical structures of three polyelectrolyte systems studied.

Characterization

Quartz Crystal Microbalance with Dissipation (QCM-D)

QCM-D is a sensitive method to measure tracer adsorption as well as viscoelasticity change of thin films in air as well as in liquid^{25,26} and it has been applied in a number of fields, including surface adsorption, surface reaction and structural change of adsorbed surface layers and so on.²⁷ QCM-D is used in the current study to measure the response of the polyelectrolyte brushes at varying salt concentration, by measuring the mass change of the brushes as well as its viscoelasticity.

One of the challenges of using QCM-D in liquid media is how to separate the frequency changes contributed from changes in mass and viscoelasticity of the adsorbed layer because, under such a condition, the traditional Sauerbrey equation cannot be used to determine the mass change.²⁸⁻³⁰

According to previous studies based on Voigt model, for QCM-D measurements in aqueous solution with both mass change

and viscoelasticity change, the frequency change (ΔF) and dissipation change (ΔD) can be expressed by the following²⁶

$$\Delta F = \text{Im} \left(\frac{\beta}{2\pi\rho_q h_q} \right), \Delta D = -\text{Re} \left(\frac{\beta}{\pi f \rho_q h_q} \right) \quad (1) \& (2)$$

$$\text{where } \beta = \xi_1 \frac{\omega\eta - i\mu}{\omega} \frac{1 - \alpha e^{2\xi_1 h}}{1 + \alpha e^{2\xi_1 h}},$$

$$\alpha = \left(\frac{\xi_1}{\xi_2} \frac{\omega\eta - i\mu}{\omega\eta_s} + 1 \right) \left(\frac{\omega\eta + i\mu}{\omega\eta_s} + 1 \right)^{-1}, \quad \xi_1 = \sqrt{-\frac{\omega^2 \rho}{\mu + i2\pi\eta}},$$

$$\xi_2 = \sqrt{i \frac{\omega\rho_s}{\eta_s}}, \text{ and the viscoelasticity of the adsorbed film is}$$

represented by a frequency-dependent complex shear modulus $\mu^* \equiv \mu' + i\mu'' = \mu + i\omega\eta$ and $\omega = 2\pi n F_0$, where ω , n and F_0 are the angular frequency, the overtone number and the fundamental resonance frequency. Symbols ρ , h and η denote the density, height and viscosity, respectively. The subscription “q” and “s” denote quartz and solvent, respectively.

For a thin viscoelastic polymer layer with its thickness smaller than the penetration depth (δ_s) of the acoustic wave into the bulk Newtonian liquid, Eq. 1 and 2 can be simplified to:²⁶

$$\Delta F_n = \left(-\frac{\eta_s}{2\pi\rho_q h_q \delta_s} \right) + \left(-\frac{\rho h \omega}{2\pi\rho_q h_q} \right) + \left(\frac{2h}{2\pi\rho_q h_q} \right) \left(\frac{\eta_s}{\delta_s} \right)^2 \left[\frac{\eta\omega^2}{\mu^2 + (\eta\omega)^2} \right] \quad (3)$$

$$\Delta D_n = \left(\frac{\eta_s}{\pi F \rho_q h_q \delta_s} \right) + \left(\frac{4h}{\rho_q h_q} \right) \left(\frac{\eta_s}{\delta_s} \right)^2 \left[\frac{\mu}{\mu^2 + (\eta\omega)^2} \right] \quad (4)$$

$$\text{where } \delta_s = (2\eta_s / \rho_s \omega)^{1/2}.$$

The first terms in Eq. 3 and 4, $\Delta F_s = -\eta_s / 2\pi\rho_q h_q \delta_s$ and $\Delta D_s = \eta_s / \pi F \rho_q h_q \delta_s$ are the contribution from the solvent.

This leads to a more simplified expression:

$$-\frac{\Delta F_n - \Delta F_s}{n} = \frac{F_0 \rho h}{\rho_q h_q} + \frac{\pi F_0^2 \eta}{\mu} n (\Delta D_n - \Delta D_s) \quad (5)$$

The two terms in the right side are the frequency change induced by mass change and viscoelasticity change of thin film, respectively.²⁷ This expression can help to discriminate the contribution from mass change and viscoelasticity change if one use it to plot $-(\Delta F_n - \Delta F_s)/n$ as a function of $n(\Delta D_n - \Delta D_s)$. By this way, values of the “actual” mass ($\rho \cdot h$) and retardation time ($\tau = \eta / \mu$) can be calculated by the intercept and the slope of the linearity.

It is noted that, for the QCM-D measurement, the deformation amplitude is about 1.0 nm, corresponding to a shear rate around 30 s⁻¹ at the fundamental frequency of 5 MHz.^{31,32} This indicates that the QCM-D measurement is in the range of linear rheological response, in which the value of modulus (μ) and viscosity (η) is constant, according to the widely used Voigt

model.^{33,34} The validity of such a data analysis is further proved in the later text.

The QCM-D measurements of the polyelectrolyte brushes in aqueous solutions were conducted with a Q-Sense E1 instrument equipped with a liquid sample cell. The AT-cut quartz crystal chips ($F_0 = 5$ MHz and sensitivity constant = $17.7 \times 10^{-9} \text{ g}\cdot\text{cm}^{-2}\cdot\text{Hz}^{-1}$) were used (Q-Sense). The surface root-mean-square roughness of the chip is less than 3.0 nm. The sample's temperature was controlled at 25°C. For all the measurements in this study, the uncertainty due to the noise was below $2 \times 10^{-9} \text{ g}\cdot\text{cm}^{-2}$.

The exchange of solution was performed using a microprocessor-controlled tubing pump (ISMATEC, IDEX, America) with a constant flow rate of $150 \mu\text{L}\cdot\text{min}^{-1}$, with *in-situ* data acquisition. When the signal stabilized, the flow was stopped and at least 5 min was allowed for sample to equilibrate, after which the data of ΔF and ΔD were collected. The solution exchange was carried out following the order from low to high salt concentration. Each step of solution exchange with one specific salt concentration was considered completed when the monitoring QCM-D signal (both frequency and dissipation) stabilized.

Ellipsometry

Thickness measurements by a spectroscopic ellipsometer (M-2000V, J. A. Woollam) were conducted at the incidence angle of 70° and the wavelength scan from 370.1 to 999.1 nm. A liquid sample cell was used for the thickness measurements in aqueous medium *in-situ*.

By ellipsometry, the complex reflection coefficient is measured as a function of wavelength expressed by the following

equation of $\tan(\Psi)e^{i\Delta} = \frac{R_p}{R_s}$, where $\tan(\Psi)$ denotes the

amplitude ratio of the reflection coefficient of p-polarized light (R_p) to that of s-polarized light (R_s), and Δ is the phase difference.³³ The quantities Ψ and Δ were measured directly in experiments and the physical parameters such as thickness and refractive index can be obtained by numerical fitting using the appropriate model. In this study, the well-established Cauchy dispersion model was used to fit the ellipsometry data³⁵ because no absorption of the incident light exists for all of the samples under investigation. By this model, the refractive index of the

substances follows the relation of $r = A + \frac{B}{\lambda^2}$, where r is the

refractive index, λ the wavelength of probing light, and A, B are two fitting parameters related to r . For the dry thickness measurements (when the brushes are not in contact with solvent), B was set as 0.01 while A was set as 1.45 for monolayer of the initiator (the self-assembled monolayer of TBP or TES). The A value was set to be 1.60 for dry PSSNa brushes.

The measurements of the samples under aqueous solutions are more complicated because of the lower optical contrast due to the decreasing in the difference of refractive index between the

brush layer and electrolyte solution. Because the salt concentration is tuned in the current study, a series of experiments were conducted to measure the refractive index of the salt solution at first. With these values measured, the measurements of polyelectrolyte brushes were performed. All measurements were conducted with the liquid sample cell and at least 15 min was allowed to let the sample equilibrate after the exchange of salt solution. Because there is no absorption of incident light by the brushes, the Cauchy dispersion relation is still valid and the numerical fitting covering a broad wavelength range helps to deduct the value of thickness and the refractive index of the polymer brushes. The validity of such a measurement is further discussed in later text.

Atomic Force Microscopy (AFM)

Besides the characterization of the swelling of the polyelectrolyte brushes by ellipsometer, separate AFM measurements were also conducted in aqueous solution. The AFM (Multimode 8, Digital Instruments) equipped with a liquid sample cell was operated in its PeakForce tapping mode where the penetration of tips into the brushes can be minimized to the best. The silicon tips on nitride cantilever (spring constant = $0.7 \text{ N}\cdot\text{m}^{-1}$) were used and the scan rate was fixed as 1.0 Hz. The brush's thickness change was monitored by measuring the step height of a scratch in the brush layer created by a blade. Prior to each measurement, the sample was incubated in NaCl solution of a specified concentration for at least 20 min to reach its equilibrated state. Special care was taken to minimize the effect of tip penetration into the brushes that may cause ambiguities in thickness determination – the setpoint value for tip engagement was kept at constantly low value for all salt concentration.

Results and discussion

Thickness of Brushes under Different Salt Levels

The grafting density (σ) is characterized by measuring the thickness of the brushes at their “dry state” (without exposure to solvents). The determination of σ value is expressed as $\sigma = N_A \rho h_{\text{dry}} / M_n$, where N_A is the Avogadro number, ρ the density of the polymer in its bulk state, h_{dry} the dry thickness of polymer brush and M_n the number average molecular weight of this polymer, respectively.² The value of the density of the bulk polymers is chosen as $1.20 \text{ g}\cdot\text{cm}^{-3}$ for PSSNa and those of both PMETAC and PSPMA are taken as $1.0 \text{ g}\cdot\text{cm}^{-3}$.³⁶ All the results and subsequent calculated parameters were listed in Table 1.

The values of thickness (h) and refractive index (r) of PSSNa, PMETAC and PSPMA brushes as a function of salt concentration (NaCl) are displayed in Figure 1a and b. For all three brush systems, their thickness values show considerable decreases at high enough salt concentration ($c_s > 0.01 \text{ M}$). These facts agree well with a number of previous studies.³⁷⁻³⁹ The most surprising feature is the moderate increases of thickness at salt concentration less than 0.01 M. For example, the h value of PSSNa brush is $\sim 29.0 \text{ nm}$ under salt free condition and it increases with the elevation of salt level and reaches $\sim 46.7 \text{ nm}$ at c_s of 0.01 M. PMETAC brushes also show

an increase from 18.1 nm to 20.5 nm for the same salt concentration range. For PSPMA brushes, its thickness changes from 7.4 nm in salt free condition to 16.7 nm at NaCl concentration of 0.1 M.

An interesting feature regarding swelling ratio from dry state is observed – for PSSNa and PMETAC brushes, which have similar value of grafting density, their swelling ratio is ~ 5.2 and 2.1, respectively, while for PSPMA brushes with a much higher grafting density (0.25 nm^{-2}), its swelling ratio is much smaller (~ 1.4). The lower swelling ratio of the more dense brush is because of the higher initial stretching of the chains by exclusive volume effect.

Table 1 Values of a few parameters of the polyelectrolyte brushes under investigation.

| Polymer | $M_n (\text{g} \cdot \text{mol}^{-1})$ | $h_{\text{dry}} (\text{nm})$ | $\sigma (\text{chain} \cdot \text{nm}^{-2})$ | $d (\text{nm})^c$ |
|---------------------|--|------------------------------|--|-------------------|
| PSSNa | 235×10^3 | 20.3 ± 2.0 | 0.06 | 4.0 |
| PSSNa | 235×10^3 | 8.4 ± 0.4 | 0.03 | 6.2 |
| PSSNa | 235×10^3 | 5.4 ± 0.4 | 0.02 | 7.8 |
| PSSNa | 60×10^3 | 12.6 ± 0.1 | 0.15 | 2.6 |
| PSSNa | 60×10^3 | 5.6 ± 0.4 | 0.07 | 3.9 |
| PMETAC ^a | 58×10^3 | 8.8 ± 0.6 | 0.09 | 3.3 |
| PSPMA ^b | 12×10^3 | 5.2 ± 0.9 | 0.25 | 2.0 |

^a M_n value was determined by NMR measurement; ^b M_n value was estimated by polymerization condition and the thickness under salt free solution; ^c Average distance between two neighboring chains.

The variation of refractive index value exhibits an opposite behavior. For PSSNa brushes, its r value experiences a decrease from 1.37 in salt free condition to 1.35 at salt concentration of 0.01 M. For PMETAC brushes, a slight decrease in r value is observed from 1.39 to 1.38 for the same salt concentration range. For PSPMA brushes, the change of r value is from 1.37 at salt free condition to 1.34 at NaCl concentration of 0.1 M.

The above data demonstrate the enhanced swelling of polyelectrolyte brushes induced by the introduction of external salt (NaCl) at moderate concentrations before the brush layer collapses at high salt level. Such swelling enhancement is also observed for the same molecular system but with different molecular weight. Figure 1c and d displays the data of PSSNa brushes of different molecular weight at similar grafting density (PSSNa-235k, $\sigma = 0.06 \text{ chain} \cdot \text{nm}^{-2}$; PSSNa-60k, $\sigma = 0.07 \text{ chain} \cdot \text{nm}^{-2}$). Both systems exhibit the increase in their thickness at NaCl concentration below 0.01 M – PSSNa-235k system thickens from 115 nm to 170 nm while the PSSNa-60k system changes from 29.0 nm to 46.7 nm. Their refractive index value decreases from 1.37 to 1.35 for the same salt concentration range. It is worthy to notice that, although the thickness values of these two systems differ from each other considerably due to different molecular weight, their refractive index values are close. This provides evidence supporting the accuracy of the ellipsometer measurements.

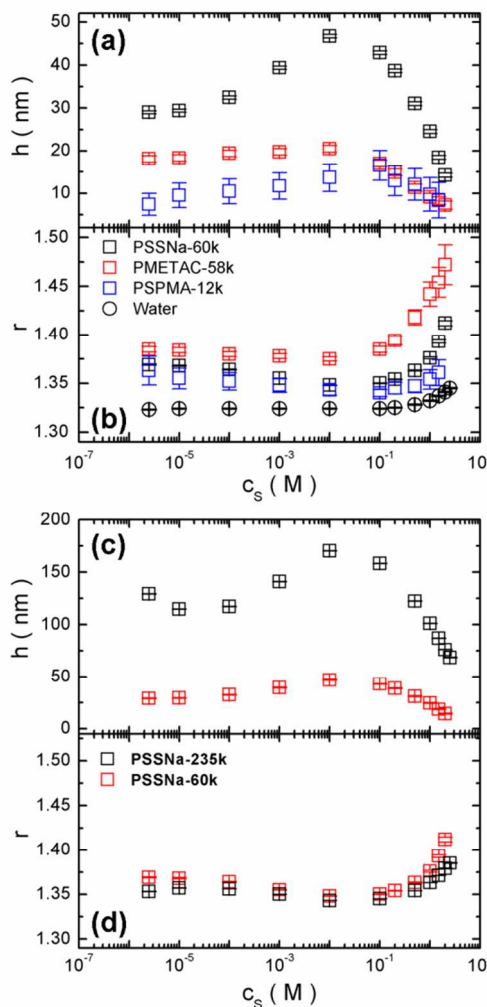


Figure 1 (a, b): Values of ellipsometric thickness (h) and refractive index (r) of three polyelectrolyte brushes as a function of salt concentration: PSSNa ($\sigma = 0.07 \text{ chain} \cdot \text{nm}^{-2}$), PMETAC ($\sigma = 0.09 \text{ chain} \cdot \text{nm}^{-2}$), PSPMA ($\sigma = 0.25 \text{ chain} \cdot \text{nm}^{-2}$). Data of refractive index of the salt solution is displayed as a comparison. (c, d): Values of thickness and refractive index of PSSNa brushes with similar grafting density but with different molecular weight as a function of salt concentration (PSSNa-235k, $\sigma = 0.06 \text{ chain} \cdot \text{nm}^{-2}$; PSSNa-60k, $\sigma = 0.07 \text{ chain} \cdot \text{nm}^{-2}$).

A parallel measurement of the swelling of PSSNa brushes (PSSNa-235k, $\sigma = 0.06 \text{ chain} \cdot \text{nm}^{-2}$) by an atomic force microscope (AFM) also exhibits the similar behavior to what measured by ellipsometer, as shown in Figure 2. Although the absolute values of the thickness measured by AFM are much smaller than those measured by ellipsometry due to the compression of the brushes by the probing tip, the enhancement of the swelling before the collapse of the brushes is obvious – the thickness measured by AFM increased from 43 nm at c_s of 10^{-5} M to 150 nm at c_s of 10^{-2} M . Compared with the data by ellipsometer, the thickness change measured by AFM is much sharper – the two sets of data exhibit a much smaller difference at c_s of 10^{-2} M than that at 10^{-5} M , showing a smaller compressibility at the state of swelling enhancement. This is attributed to the difference in inhomogeneity of the brushes

along the normal direction of the surface before and after introduction of external salt. At low salt concentration, the outer rim of the brush has a much lower segment density than the inner portion due to the dipole-dipole interaction by ion-pairs and this difference becomes smaller when the swelling is enhanced at moderate salt concentration. (A more detailed discussion will be made in later text.) When AFM tip is probing the brushes at low salt levels, the force exerted by the tip creates a bigger compression at the much less dense outer rim. When the brush is at its enhanced swelling state, the layer has a much more homogeneous distribution of segment density and therefore a more dense outer rim compared with low salt situation, generating more resistance to compression by the tip.

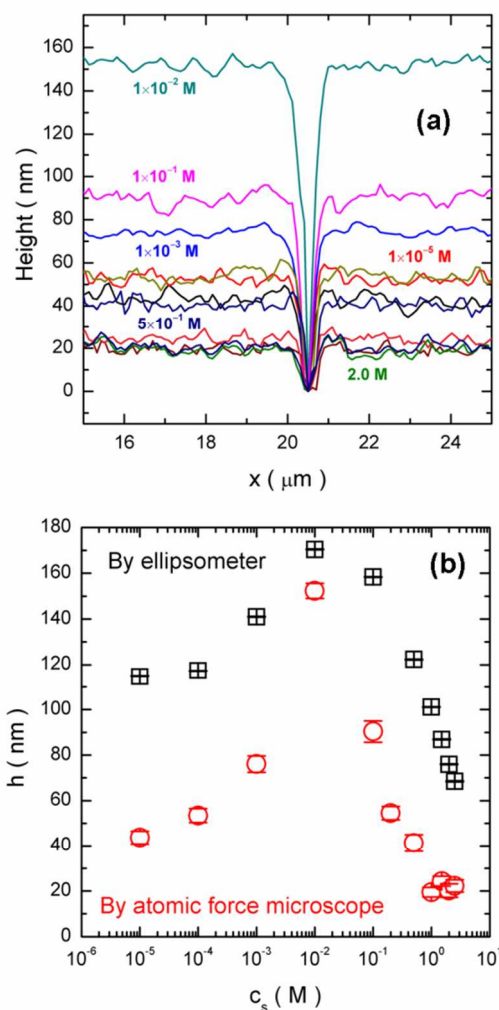


Figure 2 (a) Cross section of the scratch created inside PSSNa-235k brushes ($\sigma = 0.06$ chain- nm^{-2}) under aqueous solution with different salt concentration. The values of a few typical salt concentration are displayed in the figure. (b) Thickness of PSSNa-235k brushes ($\sigma = 0.06$ chain- nm^{-2}) measured by AFM as a function of salt concentration. The data by ellipsometry are displayed as a comparison.

The enhanced swelling is observed for PSSNa brushes with different grafting density, evidenced by the plot of thickness of swollen PSSNa brushes normalized by its degree of

polymerization, i.e. the h/N value and by its refractive index value, as a function of the grafting density (data shown in Figure 3). Clearly, both h/N and r values exhibit monotonous increase with the grafting density – an approximate linear relations is found with the r value while the h/N value experiences a saturation at higher values of grafting density. The linear increase of refractive index is a direct result of the increase of segment density with the grafting density while the saturation of the increase of h/N value shows the thickness of the brushes reaches its limited value for the full expansion of the polymer chains.

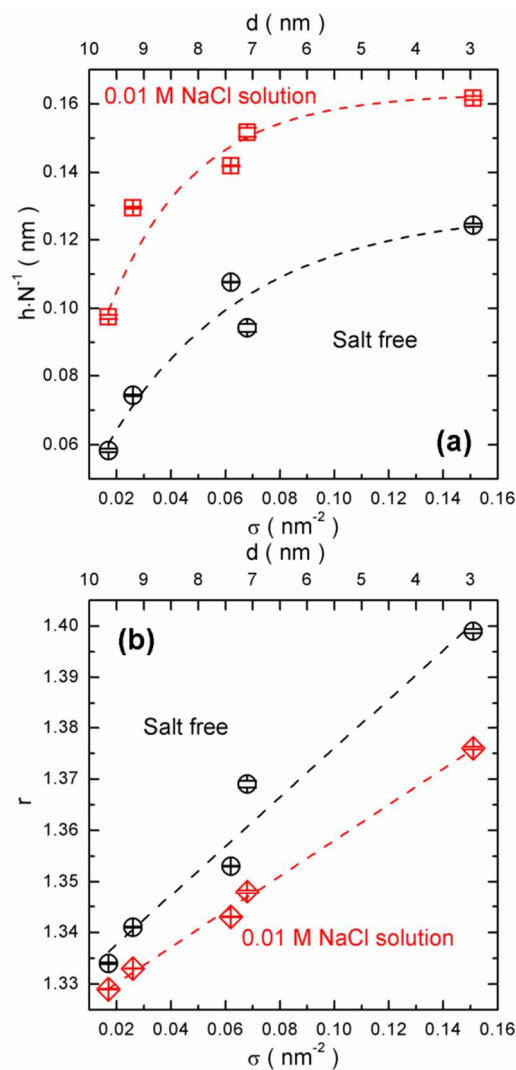


Figure 3 Values of thickness per repeat unit (a) and refractive index (b) of PSSNa brushes as a function of grafting density (and the mutual chain-chain distance) under salt free condition and in NaCl solution with concentration of 0.01 M. The dashed lines are for the guide of eyes. The first three data points from the low grafting density side are for PSSNa-235k brushes and the two at high grafting density side are for PSSNa-60k.

This experimental observation is in contrast to the prediction by scaling theory and a few previous experimental observations, in which the height of strongly charged polyelectrolyte brush is

independent on the grafting density when the brush is dense enough. Recently, it was demonstrated by a simulation⁴⁰ and an experiment⁴¹ that the excluded volume effect must be taken into account and a dependence of the brush thickness on grafting density is observed. Also, it is found that the lateral heterogeneity of the distribution of the charges can result in such a behavior.⁴⁰

The data of h/N and r with the presence of salt at moderate concentrations ($c_s < 0.01$ M) shown in Figure 3a and b demonstrate that all PSSNa brushes become more swelled (less dense) compared with the salt free situation – at NaCl concentration of 0.01 M, the values of the brush thickness are always higher than those under salt free situation while its refractive index is always lower.

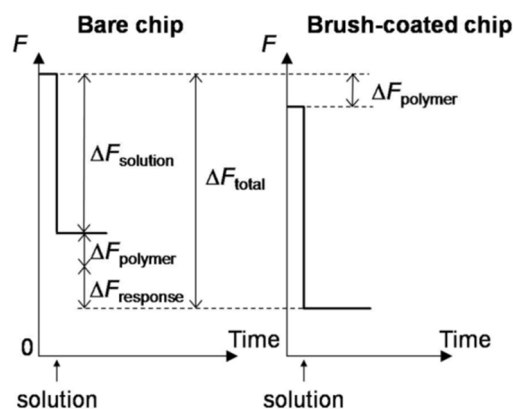
Some notes should be underlined: 1) The optical contrast between the swollen brush layer and the solution is strong enough to be detected by ellipsometer for the hydrophilic brushes with thickness in the range 10~200 nm. This can be demonstrated by the obvious least mean-squared-error fitting process as a function of thickness based on the multilayer model.⁴² (The original data and mean-squared-error fitting are provided in Supplementary Information, for three types of polyelectrolyte brushes at low salt concentration ($c_s = 2.5 \times 10^{-6}$ M) in Figure 1.) 2) The thickness and refractive index of the brushes can be separated successfully due to the spectroscopic ellipsometric measurements, in which the refractive index varies with the wavelength of incident light while the value of thickness doesn't. The determination of these two values is reliable for ellipsometry measurements covering a broad wavelength range.

Changes in Mass and Viscoelasticity of Polyelectrolyte Brushes

QCM-D was used to measure the changes in mass and viscoelasticity of the polyelectrolyte brushes to the variation of the external salt concentration. For polyelectrolyte brushes in aqueous solutions, the QCM-D's signal in frequency and dissipation should have the following contributions: the mass of the polymer, the solution, the possible ion-polymer interaction and the viscoelasticity related to change of ionic strength of the solution. Just as shown in Scheme 2, the total frequency change from that of the bare chip (ΔF_{total}) by introducing the polymer brushes and the salt solution is the summation of the contribution from mass of the polymer itself ($\Delta F_{\text{polymer}}$) and the frequency shift by the solution to the bare chip ($\Delta F_{\text{solution}}$) and the response of the brushes to the external ions ($\Delta F_{\text{response}}$), i.e.

$$\Delta F_{\text{total}} = \Delta F_{\text{polymer}} + \Delta F_{\text{solution}} + \Delta F_{\text{response}}$$
 . (The total amount of dissipation change, ΔD , has similar compositions as those of frequency changes.) When the experiments are conducted with the brush-coated chips, the frequency change from the pre-coated chip does not include the contribution from the polymer brush itself, i.e. the contribution from the polymer mass is subtracted. Therefore, the frequency change can be clearly

expressed as the summation of the contribution from the mass change inside the brushes (denoted as $\Delta F_{\text{solvent}}$) and the viscoelastic change of the brushes ($\Delta F_{\text{viscoelastic}}$), i.e. $\Delta F_{\text{total}} - \Delta F_{\text{polymer}} - \Delta F_{\text{solution}} = \Delta F_{\text{response}} = \Delta F_{\text{solvent}} + \Delta F_{\text{viscoelastic}}$. The former term on the right side of the equation is the changes in the mass of the solution inside the brushes, including the ions bound to the polymer chains and the water coupled in the brushes (to both the polymer and the ions) while the latter term comes from the changes of the polymer conformation and possible chain-chain interaction. These two parts can be well separated by analyzing the ΔF and ΔD of different overtones according to Eq. 5 – its first term of the equation gives the mass change inside the layer and the second term covers the dissipation variation, which can give an important parameter related to the viscoelasticity – the retardation time.



Scheme 2 Schematic illustration of the contributions to QCM-D signal on chips coated with polyelectrolyte brushes.

Typical data of frequency and dissipation changes of three types of polyelectrolyte brushes (PSSNa, PMETAC and PSPMA) are provided in Figure 4a, b, c and d. The data at the 3rd overtone are provided, i.e. $\Delta F_3/3$ and ΔD_3 , while the data collected at other overtones are provided in Supplementary Information. Several important features are immediately recognized: 1) In the moderate salt concentration region, all charged brushes show considerable decrease in frequency and the values increase again after reaching the minimum around the NaCl concentration of 1.0×10^{-2} - 1.0×10^{-1} M. 2) In the same concentration region for the frequency change, all brushes exhibit a peak in the dissipation value – the dissipation increases with the salt concentration and reach its maximum around the NaCl concentration between 1.0×10^{-2} and 1.0×10^{-1} M. 3) For the same type of the polyelectrolyte brushes (PSSNa brushes as the example), the thicker the layer is (higher molecular weight), the bigger frequency and dissipation changes is observed. 4) The salt concentration region of the response by the charged brushes agrees with that observed by ellipsometry, showing the accordance of the response of the charged brushes in their swelling behavior and its mass and viscoelasticity change.

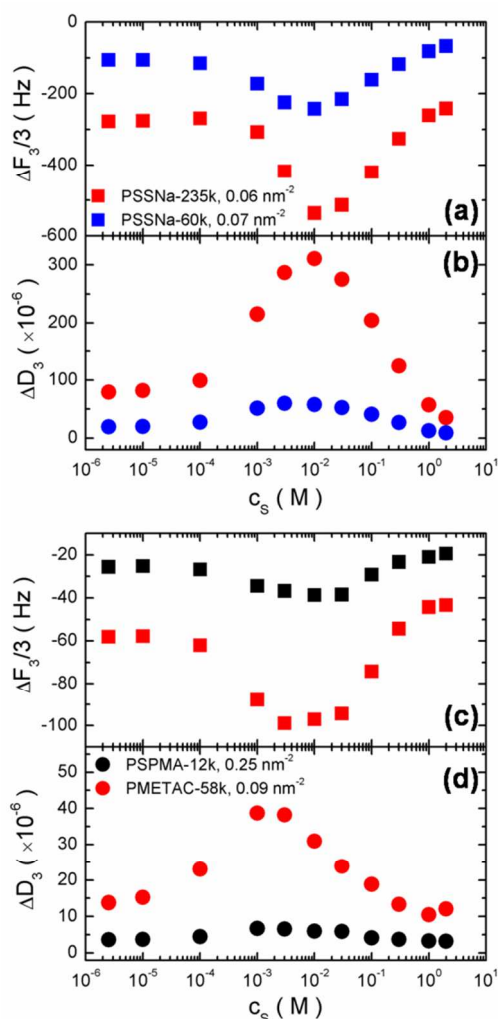


Figure 4 (a, b) Typical data of frequency and dissipation change (at 3rd overtone) of PSSNa brushes as a function of NaCl concentration. (c, d) Frequency and dissipation change of PMETAC and PSPMA brushes as a function of NaCl concentration. For PSPMA brush, KCl salt was used due to its counterions. The type, molecular weight and the grafting density of the brushes are displayed in the figures.

The response in frequency and dissipation to the variation of external salt level is the unique property of the charged brushes. This is proved by the absence of such a response of the neutral Poly(N-isopropylacrylamide) (PNIPAM) brushes – PNIPAM brush does not show any response in the similar salt concentration range and only a slight frequency increase at very high salt concentration due to the salting-out effect – also known as the lowering of the critical temperature.⁴³ (The data of PNIPAM brushes are displayed in the Supplementary Information for the sake of length of the manuscript.) One subtle point is whether the response is the result of specific interaction of the ions with the polymer, for example, the possible interaction between the ions with the phenyl group of PSSNa.⁴⁴ This is excluded by the occurrence of similar response with PSPMA brushes and PMETAC brushes, which have no phenyl in their molecular chains.

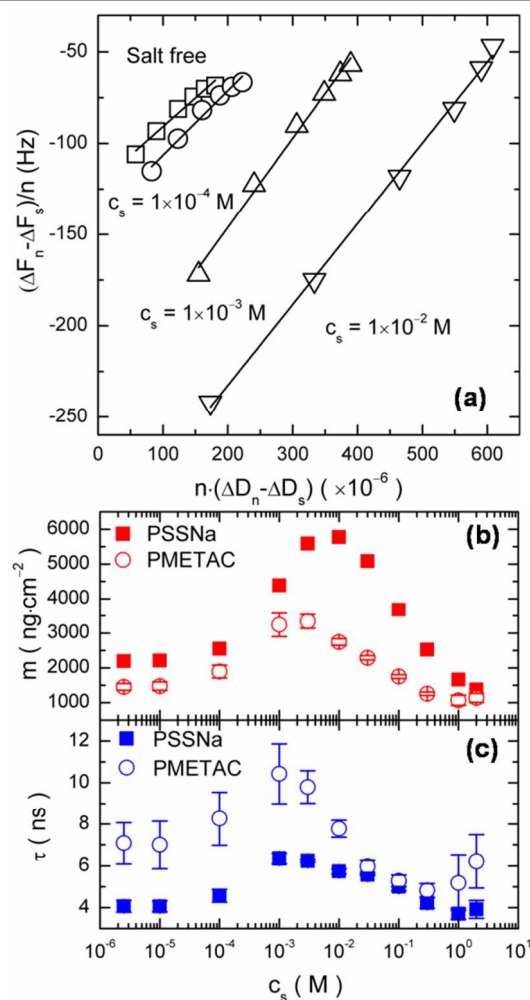


Figure 5 (a): The demonstration of the data analysis according to Eq. 5 in which the fitting of $(\Delta F_n - \Delta F_s)/n$ against $n \cdot (\Delta D_n - \Delta D_s)$ are shown by the solid lines. The data are for PSSNa-60k brushes with the grafting density of $0.07 \text{ chain}\cdot\text{nm}^{-2}$. (b) and (c): The mass of the brush layer excluding that of the polymer itself and the retardation time of the brush layer as a function of the salt concentration. The two brushes are PSSNa-60k ($\sigma = 0.07 \text{ chain}\cdot\text{nm}^{-2}$) and PMETAC-58k ($\sigma = 0.09 \text{ chain}\cdot\text{nm}^{-2}$).

Because the dissipation value of all charged brushes are quite big, the criteria of the direct use of Sauerbrey equation, i.e. $-\Delta D_n / (\Delta F_n/n) = 4 \times 10^{-7} \text{ Hz}^{-1}$, is not met.³⁴ Data analysis based on frequency spanning (Eq. 5) is conducted so that the pure contribution from the mass change can be deduced. The analysis is demonstrated in Figure 4a with the typical data for the PSSNa-60k brushes ($\sigma = 0.07 \text{ chain}\cdot\text{nm}^{-2}$) under salt solution with different concentrations. Obviously, the data agree well with the linear relation predicted by the theoretical model (Figure 5a), achieving the successful decoupling of the pure mass change from the contribution from change in viscoelasticity. Eq. 5 is an obvious step further from the results of the theoretical analysis on QCM-D using Voigt model.²⁶ By this approach and by the constitution of the frequency and dissipation response of the elastic sample shown in Scheme

^{2,29-30} the pure mass change and the viscoelastic response can be separated, by giving the mass change and the retardation time of the sample.

The value of mass and retardation time of the brushes by the numerical fittings are displayed in Figure 5b and c. (The fitting of the data with PSSNa-235k brushes is less satisfactory, and this is attributed to the effect of the big layer thickness, which is beyond the penetration depth of the acoustic wave into the solution. The data are provided in Supplementary Information.) The data show that the mass of the PSSNa brush layer increases considerably with the increase of salt concentration and it reaches the maximum value around the salt concentration of 1.0×10^{-2} M (Figure 5b). Afterwards, further increase of salt concentration leads to a decrease in mass. A similar variation of the retardation time is observed around the same salt concentration range (Figure 5c). The other two kinds of brushes show very similar responses to the external salt and the data of PMETAC brushes are provided in Figure 5b and c.

The increase of the mass inside the brush layer comes largely from the in-take of solvent (salt solution) during the swelling process. Figure 6 displays the data of mass of the PSSNa brush layer (excluding the mass of the polymer itself) as a function of salt concentration for two different grafting density values (0.07 and 0.15 chain- nm^{-2}). For comparison, the values of solvent mass calculated based on the ellipsometry data of brush's thickness and the density of the salt solution are also displayed. Clearly, the data sets show considerable similarity, despite the discrepancies at the maximum swelling.

The mass of the solvent measured by QCM-D is constantly higher than the values calculated from the thickness data. Such discrepancies are attributed to two factors: 1) The mass measured by QCM-D method should include the solvent in a layered region above the brush, which is hydrodynamically coupled to the brushes while the ellipsometer may not be sensitive enough to measure this part of contribution. 2) More water molecules are bound to the polyelectrolyte chains due to the enhancement of counterion adsorption. Increase of salt level promotes more adsorption of counterions to the charged polymer chain and more water molecules are brought to the chain as a consequence.

The increase in retardation time at the enhanced swelling indicates a change of viscoelasticity of the brushes – the brush layer gets “softer”. The data show that the value of retardation time increases from 4.1 ns and 7.1 ns at c_s of 2.5×10^{-6} M to 6.3 ns and 10.4 ns at 1.0×10^{-3} M for PSSNa and PMETAC brushes, respectively. This is a clear indication of the slowing down of the relaxation of the brushes to external strain when the salt concentration is raised from low to a moderate level. As these values of retardation time are much smaller than terminal relaxation time of charged polymer chains and much longer than the monomer relaxation time,^{32,45,46} it is believed that the retardation time measured here represents the higher relaxation modes of the polyelectrolyte chain grafted on the solid surfaces, i.e. the segmental relaxation.

All these observations demonstrate the polyelectrolyte brushes experience an enhancement of swelling induced by the

introduction of salt at moderate concentration before the brush layer shrinks at high salt levels. The enhanced swelling is expressed by the increase of its physical thickness and the decrease in its refractive index, accompanied by the increase of amount of solvent inside the brushes and the increase of the retardation time. In other words, the brush layer gets thicker, more loose, softer and heavier.

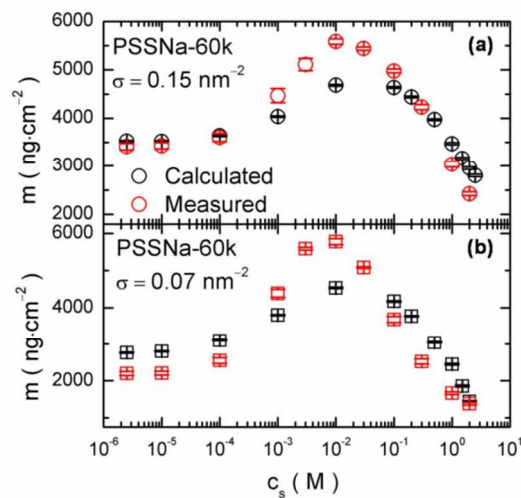


Figure 6 The comparison between the values of mass of solvent inside the PSSNa brushes measured by QCM-D and that calculated from thickness data measured by ellipsometry, as a function of salt concentration. Data for two PSSNa brushes of different grafting density are displayed: (a) 0.15 and (b) 0.07 chain- nm^{-2} .

What is the mechanism of the swelling enhancement? The phenomenon indicates more stretching of the permanently charged polymer chains inside the brushes by the increase of salt concentration, compared with the salt free situation. Such a behavior is counter-intuitive considering the well-known properties of permanently charged polyelectrolytes, whose molecular dimension reduces upon the increase of external salt concentration, as a result of the enhanced counterion adsorption.^{47,48}

Compared with polyelectrolyte chains dissolved in solutions, polyelectrolyte brushes bring extremely high surface charge density by its high density of charged segments. The strong electrostatic attraction makes a large amount of counterions reside inside the brush layer so that the original charges are partially or largely neutralized.^{5,16} Such a high concentration of charges and their counterions inside the brushes can bring about the formation of numerous ion-pairs.⁴⁹

Based on this fact, a scenario is proposed to explain the swelling enhancement of polyelectrolyte brushes – the penetration of external ions break up the multiplets formed by the ion-pairs.⁵⁰ The densely confined charges and counterions inside the brushes bring about the formation of the ion-pairs and the resulted dipole-dipole interaction between the ion-pairs makes them bound together, forming multiplets,⁵⁰ which partly restrict the complete stretching of the polymer chains in the brushes.⁵¹ Such a behavior is analogy to previous observation in

polyelectrolyte gels, in which the enthalpy-favored formation of multiplets serves as the physical cross-links.^{51,52} When external salt is introduced, additional ions are driven into the brushes and the previous dipole-dipole interaction by ion-pairs is disrupted and the multiplets break up. As a consequence, the previously bound segments by the multiplets are therefore de-bound, making the polyelectrolyte chain more stretched and resulting in the promotion of the swelling of the brushes. This process is similar to the anti-polyelectrolyte effect of polyzwitterions, which changes from the insoluble state to the soluble one when the interaction between the permanent dipoles is broken up by the introduction of external ions in aqueous media.^{53,54} A schematic illustration of the scenario of the enhanced swelling is displayed in Figure 7.

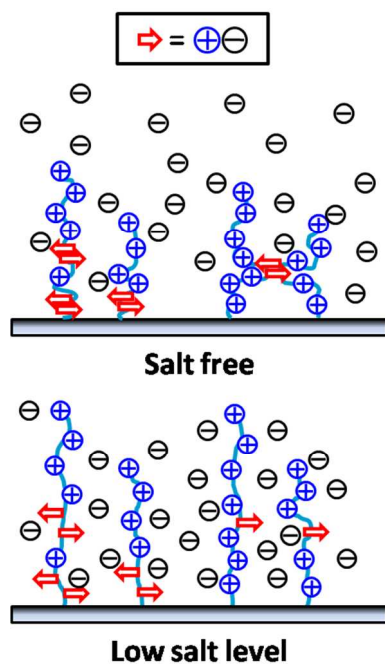


Figure 7 The schematic illustration of the proposed physical model of the enhanced swelling of polyelectrolyte brushes induced by the introduction of external ions – the previously existing dipole-dipole interaction inside the brush is broken up by the penetration of counterions. The red arrows denote the dipole formed by ion-pairs.

A few notes should be made compared with a few previous investigations. 1) The thickness change of polyelectrolyte brushes in response to the change of external salt concentration has been studied intensively with different methods including neutron reflectivity,^{14,19} X-ray reflectivity,^{55,56} surface force apparatus³⁸ and ellipsometry.^{15,39} Lots of attention was paid to the collapse of the brushes at high salt concentration. At lower salt concentration region, there have been different observations – some indicate no change of thickness with salt concentration while some studies demonstrate increases in thickness, similar with what observed in the current study. Among the methods mentioned, the reflectivity and ellipsometry measurements are considered to be the most intact. In this sense, a very recent observation using neutron reflectivity shows similar moderate thickness increase with a permanently charged polyelectrolyte

brush system.¹⁴ 2) For weak polyelectrolyte brushes whose charge density depends on the association-dissociation balance of the ionizable groups, the enhanced swelling has been observed with moderate increase of salt concentration, as described in the Introduction. The physical mechanism is proved to be the enhancement of ionization due to the local pH change and ion exchange process.⁵⁷ This is principally different to what observed in the current study, in which all of the polyelectrolyte chains are permanently charged and never depends on the pH value of the solution.

Conclusions

With a combination of methods, including ellipsometry, QCM-D and AFM, the ion-induced enhancement of swelling of a few polyelectrolyte brushes is discovered. Upon the elevation of salt concentration (NaCl), the brush thickness increases before it shrinks at high enough salt concentration. Accompanying the thickness' increase, there observed the decrease of refractive index, the mass increase inside the brushes and the increase of retardation time – the brushes get thicker, less dense and softer. The mechanism is proposed as the penetration of ions into the brushes driven by the increase of external salt level and the ions disrupt and break the previously formed dipole-dipole interaction, releasing the segments bound together and stretching the polymer chains.

Acknowledgements

This research is supported by the National Natural Science Foundation of China (NSFC 51173197, 20925416).

Notes and references

^a Beijing National Laboratory for Molecular Science, Institute of Chemistry, Chinese Academy of Sciences, Beijing 100190, China. Email: jzhao@iccas.ac.cn

^b Also affiliated with the Graduate University of Chinese Academy of Sciences, Beijing 100049, China.

^c Department of Chemical Physics, Hefei National Laboratory for Physical Sciences at the Microscale, University of Science and Technology of China, Hefei 230026, China.

Electronic Supplementary Information (ESI) available. See DOI: 10.1039/b000000x/

- H. B. Bohidar, P. Dubin and Y. Osada, *Polymer Gels Fundamentals and Applications*, Oxford University Press, Washington, 2003.
- R. Barbey, L. Lavanant, D. Paripovic, N. Schüwer, C. Sugnaux, S. Tugulu and H. Klok, *Chem. Rev.*, 2009, **109**, 5437.
- Y. Qiu and K. Park, *Adv. Drug Deliv. Rev.*, 2001, **53**, 321.
- R. Advincula, W. J. Brittain, K. C. Caster and J. Rühle, *Polymer Brushes Synthesis, Characterization, Application*, WILEY-VCH Verlag GmbH & Co. KGaA, Weinheim, 2004.
- Pincus, P. *Macromolecules*, 1991, **24**, 2912.
- U. Raviv, S. Giasson, N. Kampf, J. F. Gohy, R. Jérôme and J. Klein, *Nature*, 2003, **425**, 163.
- A. Wittemann, B. Haupt and M. Ballauff, *Phys. Chem. Chem. Phys.*, 2003, **5**, 1671.
- E. P. K. Currie, A. B. Sieval, G. J. Fleer and M. A. Cohen Stuart, *Langmuir*, 2000, **16**, 8324.
- T. Wu, P. Gong, I. Szleifer, P. Vlček, V. Šubr and J. Genzer, *Macromolecules*, 2007, **40**, 8756.

- 10 B. Lego, W. G. Skene and S. Giasson, *Macromolecules*, 2010, **43**, 4384.
- 11 M. Biesalski, D. Johannsmann and J. R  he, *J. Chem. Phys.*, 2002, **117**, 4988.
- 12 J. D. Willott, T. J. Murdoch, B. A. Humphreys, S. Edmondson, G. B. Webber and E. J. Wanless, *Langmuir*, 2004, **30**, 1827.
- 13 E. B. Zhulina, T. M. Birshtein and O. V. Borisov, *Macromolecules*, 1995, **28**, 1491.
- 14 I. E. Dunlop, R. K. Thomas, S. Titmus, V. Osborne, S. Edmondson, W. T. S. Huck and J. Klein, *Langmuir*, 2012, **28**, 3187.
- 15 M. Biesalski, D. Johannsmann and J. R  he, *J. Chem. Phys.*, 2004, **120**, 8807.
- 16 M. Ballauff and O. Borisov, *Curr. Opin. Colloid Interface Sci.*, 2006, **11**, 316.
- 17 Y. Tran, P. Auroy, L. T. Lee and M. Stamm, *Phys. Rev. E*, 1999, **60**, 6984.
- 18 O. Azzaroni, A. A. Brown and W. T. S. Huck, *Adv. Mater.*, 2007, **19**, 151.
- 19 Y. Tran, P. Auroy and L. T. Lee, *Macromolecules*, 1999, **32**, 8952.
- 20 Y. Hou, G. Liu, Y. Wu and G. Zhang, *Phys. Chem. Chem. Phys.*, 2011, **13**, 2880.
- 21 C. Zhang, X. Chu, Z. Zheng, P. Jia and J. Zhao, *J. Phys. Chem. B*, 2011, **115**, 15167.
- 22 Y. Tran and P. Auroy, *J. Am. Chem. Soc.*, 2001, **123**, 3644.
- 23 M. Kobayashi, M. Terada, Y. Terayama, M. Kikuchi and A. Takahara, *Macromolecules*, 2010, **43**, 8409.
- 24 G. Masci, D. Bontempo, N. Tiso, M. Diociaiuti, L. Mannina, D. Capitani and V. Crescenzi, *Macromolecules*, 2004, **37**, 4464.
- 25 G. Sauerbrey, *Z. Phys.*, 1959, **155**, 206.
- 26 M. V. Voinova, M. Rodahl, M. Jonson and B. Kasemo, *Phys. Scr.*, 1999, **59**, 391.
- 27 F. H  k, B. Kasemo, T. Nylander, C. Fant, K. Sott and H. Elwing, *Anal. Chem.*, 2001, **73**, 5796.
- 28 L. Fu, X. Chen, J. He, C. Xiong, and H. Ma, *Langmuir*, 2008, **24**, 6100.
- 29 Y. Zhang, B. Du, X. Chen and H. Ma, *Anal. Chem.*, 2009, **81**, 642.
- 30 L. Fu, Y. Chen and H. Ma, *Macromol. Rapid Commun.*, 2012, **33**, 735.
- 31 F. H  k, M. Rodahl, P. Brzezinski and B. Kasemo, *Langmuir*, 1998, **14**, 729.
- 32 D. Boris and R. H. Colby, *Macromolecules*, 1998, **31**, 5746.
- 33 P. Oswald, *Rheophysics-The Deformation and Flow of Matter*, Cambridge University Press, Cambridge, 2009.
- 34 I. Reviakine, D. Johannsmann and R. P. Richter, *Anal. Chem.*, 2011, **83**, 8838.
- 35 H. Fujiwara, *spectroscopic ellipsometry principles and applications*, Maruzen Co. Ltd, Tokyo, 2003.
- 36 Z. Adamczyk, M. Zembala, P. Warszyński, B. Jachimska, *Langmuir*, 2004, **20**, 10517.
- 37 H. Ahrens, S. F  rster and C. A. Helm, *Phys. Rev. Lett.*, 1998, **81**, 4172.
- 38 M. Balastre, F. Li, P. Schorr, J. Yang, J. W. Mays and M. V. Tirrell, *Macromolecules*, 2002, **35**, 9480.
- 39 S. Sanjuan, P. Perrin, N. Pantoustier and Y. Tran, *Langmuir*, 2007, **23**, 5769.
- 40 C. Seidel, *Macromolecules*, 2003, **36**, 2536.
- 41 G. Romet-Lemonne, J. Daillant, P. Guenoun, J. Yang and J. W. Mays, *Phys. Rev. Lett.*, 2004, **93**, 148301.
- 42 *CompleteEASE Data Analysis Manual*, J. A. Woollam Co., Inc., Lincoln, 2009.
- 43 Y. K. Jhon, R. R. Bhat, C. Jeong, O. J. Rojas, I. Szleifer and J. Genzer, *Macromol. Rapid Commun.*, 2006, **27**, 697.
- 44 J. C. Ma and D. A. Dougherty, *Chem. Rev.*, 1997, **97**, 1303.
- 45 R. H. Colby, D. C. Boris, W. E. Krause and S. Dou, *Rheol. Acta.*, 2007, **46**, 569.
- 46 P. G. de Gennes, *Scaling concepts in polymer physics*, Cornell University Press, Ithaca, 1979.
- 47 M. Muthukumar, *J. Chem. Phys.*, 2004, **120**, 9343.
- 48 P. Jia, Q. Yang, Y. Gong and J. Zhao, *J. Chem. Phys.*, 2012, **136**, 084904.
- 49 R. Kumar, B. Sumpter and M. Kilbey, *J. Chem. Phys.*, 2012, **136**, 234901.
- 50 K. A. Mauritz, *J. Macromol. Sci., Rev. Macromol. Chem. Phys. C*, 1988, **28**, 65.
- 51 E. Yu. Kramarenko, O. E. Philippova and A. R. Khokhlov, *Polymer Sci., Ser. C*, 2006, **48**, 1.
- 52 S. G. Starodoubtsev, A. R. Khokhlov, E. L. Sokolov and B. Chu, *Macromolecules*, 1995, **28**, 3930.
- 53 M. Kobayashi, Y. Terayama, M. Kikuchi and A. Takahara, *Soft Matter*, 2013, **9**, 5138.
- 54 A control experiment measuring the physical adsorption of PSSNa chains to the solid substrates helps to exclude the possible contribution from physis-adsorption – only a tracer amount of adsorption is observed.
- 55 P. Guenoun, A. Schlachli, D. Sentenac, J. W. Mays and J. J. Benattar, *Phys. Rev. Lett.*, 1995, **74**, 3628.
- 56 P. Kaewsaiha, K. Matsumoto and H. Matsuoka, *Langmuir*, 2004, **20**, 67
- 57 54.H. Zhang and J. R  he, *Macromolecules*, 2005, **38**, 4855.